PHYSICAL REVIEW A **69**, 023202 (2004)

Shell structure in mixed ^{3}He-^{4}He droplets

J. Navarro
IFIC (CSIC-Universidad de Valencia), Edificio Institutos de Paterna, Apartado Postal 22085, E-46071 Valencia, Spain

A. Poves
Departamento de Física Teórica, Universidad Autónoma de Madrid, E-28049 Madrid, Spain

M. Barranco and M. Pi
Departament d'Estructura i Constituents de la Matèria, Facultat de Física, Universitat de Barcelona, E-08028 Barcelona, Spain

(Received 12 November 2003; published 18 February 2004)

Due to the immiscibility of ^{3}He into ^{4}He at very low temperatures, mixed helium droplets consist of a core of ^{4}He atoms coated by a ^{3}He layer whose thickness depends on the number of atoms of each isotope. When these numbers are such that the centrifugal kinetic energy of the ^{3}He atoms is small and can be considered as a perturbation to the mean-field energy, a novel shell structure arises, with magic numbers different from these of pure ^{3}He droplets. If the outermost shell is not completely filled, the valence atoms align their spins up to the maximum value allowed by the Pauli principle.

DOI: 10.1103/PhysRevA.69.023202 PACS number(s): 36.40.−c, 61.25.Bi, 67.60.−g

I. INTRODUCTION

In the last few years the study of liquid-helium droplets has attracted a renewed interest. The main reason for this has been the observation first made by Scoles and collaborators [1] of the ν_3 vibrational band of SF_6 dissolved in ^{4}He droplets. Since then, a major effort has been made to address the infrared spectroscopy of molecules inside or attached to helium clusters [2–4]. In a millisecond time scale [5], liquid-helium droplets cool down to temperatures below 0.4 K in the case of ^{4}He and 0.15 K in the case of ^{3}He [2,5,6]. The unexpectedly sharp rotational lines observed in the infrared spectral region when molecules such as SF_6 and OCS [2,7] are inside a ^{4}He drop have been interpreted as a signature of the ^{4}He drop superfluidity [8]. On-flight cold ^{4}He droplets may thus offer the unique possibility of resolving rotational spectra of complex molecules, acting as an inert spectroscopic matrix [9] with potential applications in basic and applied research. The situation found when the same molecular impurities are dissolved into ^{3}He droplets is at variance: in these fermionic drops the atoms are in the normal state, the rotational lines collapse, and the infrared spectrum shows only one broad peak [8]. The structure and collective excitations of ^{3}He droplets doped with atomic and molecular impurities have been recently addressed [10].

The study of mixed ^{3}He-^{4}He drops is very appealing. They are made of bosons and fermions with different mass interacting through the same potential, and quantum effects due to the different statistics and the different zero-point motion of each isotope are crucial to determine their structure. Moreover, there is a practical motivation in their study since, as compared to pure ^{4}He droplets, mixed ^{3}He-^{4}He droplets may provide an even cooler environments to dopant molecules [11]. Indeed, evaporation from the outer layers of ^{3}He brings the temperature of the compound system down to values close to those of pure ^{3}He drops, while keeping superfluid the inner helium layers around the foreign molecule, as these layers are essentially made of ^{4}He atoms, provided there is enough of this isotope to fill the first two solvation shells around the impurity [12]. Doped mixed ^{3}He-^{4}He droplets have also found an application in basic research, giving an experimental answer to the question of how many ^{4}He atoms are needed to exhibit superfluid behavior. Theoretical calculations [13,14] predicted a value around 60, in excellent agreement with the recent experimental findings of Toennies and co-workers [8], on what they have called ''molecular superfluidity'' (see however Ref. [15] for an alternative explanation).

Pure ^{3}He droplets are finite systems made of the only neutral Fermi liquid accessible to experiments, and since these atoms are fermions, they are believed to be distributed into shells. For some number of atoms (magic numbers), the droplets have a particularly stable structure, as inert atoms or doubly magic atomic nuclei—such as ^{16}O or ^{208}Pb—have. Experimental evidence about the existence of magic numbers has also been gathered for other fermionic systems, such as alkali-metal clusters [16] and quantum dots [17]. Although there is no experimental evidence of the existence of magic numbers in ^{3}He droplets, all calculations carried out so far yield for the first magic numbers the sequence $(p+1)(p+2)(p+3)/3$ with $p=0,1,2,\ldots$ characteristic of the three-dimensional harmonic-oscillator (HO) well [18–21].

Whereas any number of ^{4}He atoms can form a self-bound system, a minimum number N_0 is needed in the case of ^{3}He [18,19,22–24]. The precise value of N_0 has not been experimentally determined, but the fact that only large ^{3}He clusters suddenly appear in the experiments points towards its existence. The pioneering calculations of Refs. [18,19] concluded that N_0 should be comprised between 20 and 40, which are the magic numbers corresponding to $p=2$ and 3 in the HO scheme. The value $N_0=29$ has been obtained [22] in a configuration interaction plus density-functional description of ^{3}He droplets, whereas the value $N_0=34-35$ has been found in variational Monte Carlo (VMC) calculations [23,24]. According to Ref. [22] a salient feature of the open shell droplets spanning the $20<N<40$ range is that the va-

lence atoms couple their spins to the maximum value allowed by the Pauli principle. This is a surface effect—bulk liquid ^{3}He in its ground state is unpolarized—also found in VMC calculations [23,24]. The atoms in the inner, closed shells, couple their spins so as to yield a paramagnetic, zero-spin configuration.

In this work we address the shell structure of the fermionic component in a cold, mixed helium droplet when the number of ^{4}He atoms N_4 is much larger than the number of ^{3}He atoms N_3. The presence of ^{4}He atoms produces two effects. On the one hand, they provide an extra binding to the ^{3}He system, which may be crucial to have bound small mixed droplets, as shown by recent microscopic calculations [25–27]. On the other hand, they change the mean field where ^{3}He atoms move, drastically affecting the shell structure and magic numbers of the ^{3}He component. To highlight shell effects that otherwise will be smeared out, the more interesting situation corresponds to fairly small N_3 values. As cases of study we consider two (N_3,N_4) systems fulfilling these conditions, namely, the (50,300) and (288,1440) droplets.

This paper is organized as follows. In Sec. II we present a mean-field description of mixed helium droplets based on a finite-range density-functional approach. In Sec. III we go beyond the mean-field description taking into account the mixing of configurations within a shell-model approach, and a summary is presented in Sec. IV.

II. MEAN-FIELD DESCRIPTION

In this study we have employed the finite-range density functional (FRDF) of Ref. [28]. This functional reproduces the relevant thermodynamical properties of ^{4}He and ^{3}He liquids at zero temperature, such as the equations of state and the surface tension of the free surfaces, and properties of the mixture such as maximum solubility of ^{3}He into ^{4}He, pressure and concentration dependence of ^{3}He effective mass, excess volume coefficient, osmotic pressure, and surface tension of the mixture interface as a function of pressure.

For a given droplet we have solved self-consistently the coupled integrodifferential equations arising from functional differentiation of the density functional [28]. The Euler-Lagrange equation obeyed by the spherically symmetric ^{4}He particle density $\rho_4(r)$ can be written as

$$\left[-\frac{\hbar^2}{2m_4}\left(\frac{d^2}{dr^2}+\frac{2}{r}\frac{d}{dr}\right)+V_4(r)\right]\sqrt{\rho_4(r)}=\mu_4\sqrt{\rho_4(r)}, \tag{1}$$

where μ_4 is the ^{4}He chemical potential. The ^{3}He spherical orbitals $\phi_{nl}(r)$ are solution of the Kohn-Sham-like (KS) equations

$$\left[-\frac{\hbar^2}{2m_3^*}\left(\frac{d^2}{dr^2}+\frac{2}{r}\frac{d}{dr}\right)-\frac{d}{dr}\left(\frac{\hbar^2}{2m_3^*}\right)\frac{d}{dr}\right]\phi_{nl}(r)$$
$$+\left[V_3(r)+\frac{\hbar^2}{2m_3^*}\frac{l(l+1)}{r^2}\right]\phi_{nl}(r)=\varepsilon_{nl}\phi_{nl}(r), \tag{2}$$

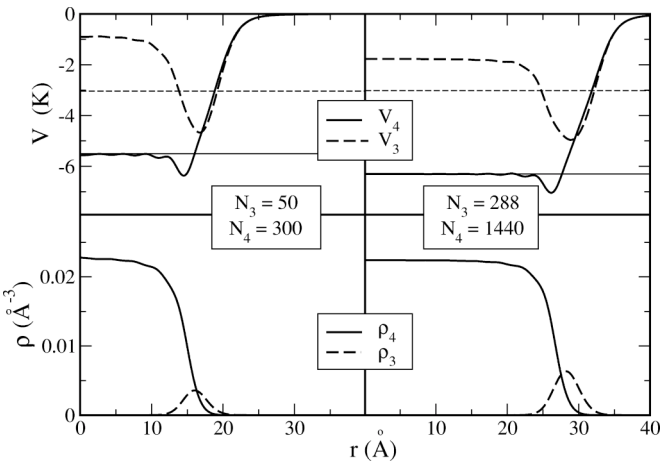

FIG. 1. Effective SP potentials V_4 and V_3 (upper panels) and densities ρ_4 and ρ_3 (lower panels) for the drops with $N_3=50$, $N_4=300$ atoms (left side) and $N_3=288$, $N_4=1440$ atoms (right side). The horizontal dashed and solid lines in the upper panels represent the ^{3}He and ^{4}He chemical potentials, respectively.

where ε_{nl} are the single-particle (SP) energies, and n and l are the radial and orbital angular-momentum quantum numbers, respectively. Within FRDF theory, the effective potentials V_4 and V_3, and the effective mass m_3^* depend on the atomic densities ρ_4 and ρ_3.

The key point for our discussion is that the resulting effective potential V_3 is small and flat except for a very pronounced pocket at the surface of the drop and, as a consequence, the low-lying ^{3}He SP states are localized at the surface. This situation has been analyzed in detail for one single ^{3}He impurity in a ^{4}He droplet [29–31]. The surface potential well arises from the balance between the atom-atom interaction, which binds the ^{3}He atom to the droplet, and the excess of kinetic energy of one ^{3}He atom with respect to that of one ^{4}He atom, which tends to push the ^{3}He atom off the droplet. This is the origin of the well-known Andreev surface states.

It turns out that V_3 has a fairly large number of bound SP surface states, therefore a ^{3}He layer can develop at the surface of the ^{4}He component, forming a quasi-two-dimensional spherical shell. This is illustrated in Fig. 1 for the two drops we have chosen as typical examples. In the upper panels we have plotted the effective potentials V_4 and V_3. All ^{3}He atoms occupy surface states, and this is clearly reflected in the ρ_3 density as displayed in the lower panels of the figure. We have found that this is always the pattern if N_3 is small enough as compared with N_4. The maximum number of ^{3}He atoms which can be accommodated in a single shell on the surface of a ^{4}He drop can be roughly estimated as $4\pi R^2\Delta r\rho_3$, where $R\simeq 3N_4^{1/3}$ Å is the radius of the ^{4}He drop, $\Delta r\simeq 2$ Å is the "diameter" of a ^{3}He atom, and $\rho_3\simeq 0.016$ Å^{-3} is the bulk ^{3}He density. The surface of the drop can thus accommodate all the ^{3}He atoms if the condition $N_3\leqslant 3.5N_4^{2/3}$ is fulfilled. It appears that only for rather small N_4 values, ^{3}He has a sizable probability of being dissolved in the bulk of the droplet. A discussion on how ^{3}He dissolves in ^{4}He droplets can be found in Ref. [12].

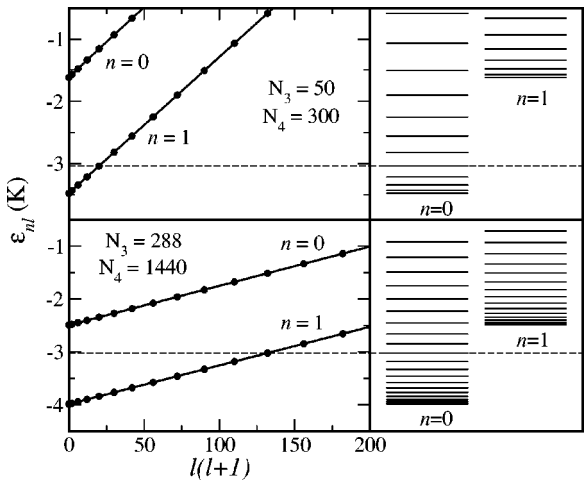

FIG. 2. ^{3}He SP energies ε_{nl} as a function of $l(l+1)$. The dashed horizontal lines represent the ^{3}He chemical potential.

The fact that the effective potential V_3 has a pronounced minimum at the surface of the mixed drop has interesting consequences for the ^{3}He shell structure. If the radius R, i.e., N_4, is large enough, the centrifugal term $l(l+1)/r^2$ entering the KS equations can be treated as a perturbation. The unperturbed SP orbitals do not depend on the orbital angular momentum l, and in first-order perturbation theory the SP energies would vary linearly with $l(l+1)$, giving rise to a rotational spectrum. This simple picture is indeed confirmed by the solution of the KS equations, as can be seen in Fig. 2, where we display the SP energies as a function of $l(l+1)$. They are distributed in two nearly parallel straight lines, one corresponding to the nodeless $n=0$ states and the other to the $n=1$ states. The slope of these lines, as well as the gap between the last occupied $n=0$ and the first unoccupied $n=1$ sp state, diminish as N_4 increases. The corresponding SP wave functions $\phi_{nl}(r)$ are plotted in Fig. 3. It is worth noticing that the $n=0$ wave functions are almost indistinguishable from each other, and even the $n=1$ ones in the larger droplet. A similar situation has been found for single ^{3}He impurities diluted in ^{4}He adsorbed in the interior of carbon nanotubes [32], and for edge ^{3}He states in a ^{4}He drop on a Cs surface [33]. The rotational character of the spectrum of *one* single ^{3}He atom in a ^{4}He droplet has been previously discussed in Refs. [29,31].

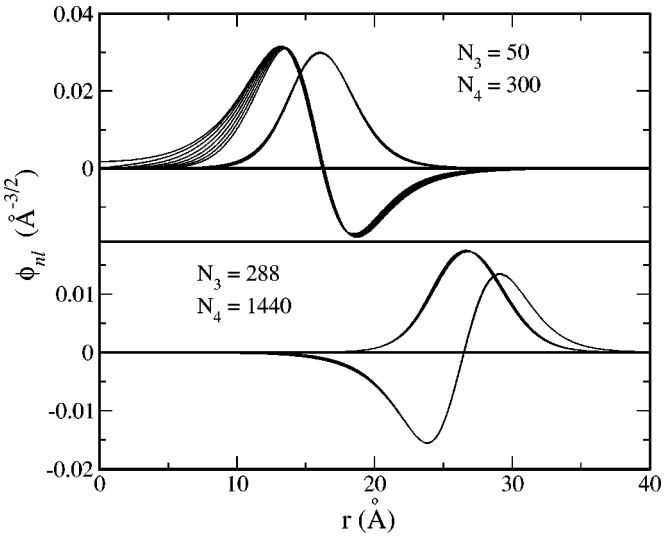

FIG. 3. Upper panel: ^{3}He SP radial wave functions with $n=0$ and $n=1$ as a function of r for drops with $N_3=50$, $N_4=300$. Lower panel: the same as the upper one for $N_3=288$, $N_4=1440$. For each n value, the first 14 wave functions have been plotted.

We thus see that there are two energy scales clearly separated. The large one is related to the number of nodes of the radial wave function and the small one to the different values of the orbital angular momentum for a given number of nodes. Therefore, when $N_4 \gg N_3$ the ^{3}He mean field gives rise to a distinct shell structure in which the SP energy levels group into rotational bands whose head states ϕ_{n0} are characterized by the number of nodes of their radial wave function. For drops satisfying the condition $N_3 \leqslant 3.5N_4^{2/3}$, the Fermi level corresponds to an $n=0$, nodeless orbital; the $n=1$ SP states lie at higher energies. It can be seen in Fig. 2 that the $n=1$ band crosses the $n=0$ band at $l_{cr}=8$ for $N_4=300$ and at $l_{cr}=14$ for $N_4=1440$. The total number of atoms that can be placed in the $n=0$ bands up to l_{cr} is 162 and 450, respectively $[N_3=2\Sigma_0^{l_{cr}}(2l+1)=2(l_{cr}+1)^2]$. These numbers are in very good agreement with the estimates given by the above inequality. We thus conclude that, as far as the inequality is respected, new magic numbers $N_3=2(p+1)^2$ appear, with $p=0,1,\ldots,l_{cr}$.

III. BEYOND MEAN FIELD

To study the behavior of these mixed droplets beyond the mean-field approximation we proceed along the same lines as in Ref. [22]. The starting point is the calculation of the two-body matrix elements of the residual interaction between SP states characterized by l_i and l_j (or l_m and l_n), coupled to orbital angular momentum L and spin S,

$$V_{ijmn}^{LS}=\langle l_i,l_j;LS|V|l_m,l_n;LS\rangle. \tag{3}$$

As residual interaction we take the effective interaction deduced from the finite-range density functional employed in preceding section. The SP wave functions obtained in the mean-field calculation are expanded in an optimized HO basis, to take advantage of the Brody-Moshinsky transformation brackets [34] in the calculation of the antisymmetrized two-body matrix elements. In what follows we shall use the wave functions of the (50,300) droplet. We have computed the matrix elements V_{ijmn}^{LS} for SP angular moments $l=0-6$. In Table I are displayed the diagonal matrix elements V_{ijij}^{LS} pertaining to the l shells at and above the Fermi level. The behavior of the other matrix elements is qualitatively similar.

In a single l shell, the fermionic character of the ^{3}He atoms together with the repulsion at short distances of the atom-atom interaction produces positive matrix elements in the $S=0$ channel, the largest one corresponding to $L=0$. The average $S=0$ interaction is close to zero but slightly positive (+3 mK). On the contrary, the attraction manifests

TABLE I. Antisymmetrized two-body matrix elements $\langle l_i, l_j; L, S|V|l_m, l_n; LS\rangle$ in mK for the (50,300) droplet.

l_i	l_j	l_m	l_n	L	$S=0$	L	$S=1$
4	4	4	4	0	+83	1	−67
				2	+11	3	−26
				4	+6	5	−16
				6	+1	7	−10
				8	−11		
4	5	4	5	1	+111	1	−81
				2	−17	2	−80
				3	+30	3	−8
				4	−3	4	−47
				5	+15	5	−2
				6	−1	6	−32
				7	+5	7	−1
				8	0	8	−23
				9	−21	9	−2
5	5	5	5	0	+142	1	−93
				2	+18	3	−38
				4	+12	5	−24
				6	+7	7	−18
				8	+3	9	−13
				10	−11		

in the $S=1$ channel (odd-L values) and it is dominated by the $L=1$ matrix element (≈ -100 mK). The average attraction in this channel is -25 mK. Actually, the odd-L matrix elements behave exactly as those of an attractive δ interaction for even L, i.e., as $(2L+1)^{-1}$, while the $S=0$, even-L elements are very close to those of a (repulsive) BCS-like pairing interaction, as can be seen in Fig. 4, where the diagonal matrix elements in the $l=5$ shell are displayed. The gross features of these matrix element are the same that appear in the study of pure ^{3}He droplets although their size and detailed structure are different. Matrix elements involving two different l shells show similar features, $S=0$ repulsion and $S=1$ attraction, more prominent for the smaller L values.

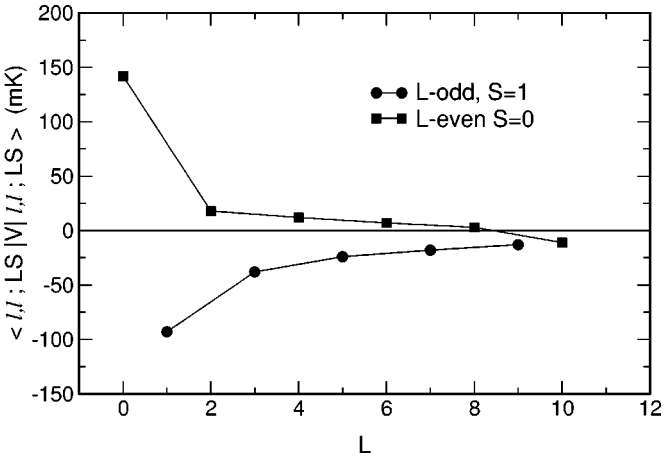

FIG. 4. Diagonal two-body matrix elements of the effective interaction in the $l=5$ shell for the (50,300) droplet.

When we fill orderly the l shells for a nonmagic number of atoms, the valence atoms—those outside closed shells—may be described by many different Slater determinants that are degenerate in energy at the mean-field description level. The residual interaction mixes them all to produce the physical ground and excited states. We have resorted to a configuration interaction calculation in the valence l shell to determine them. Even without diagonalizing the secular matrices, we can guess that the interaction will favor states with maximum spin, because it is attractive in the $S=1$ channel and repulsive in the $S=0$ channel. Indeed, this is the result that we obtain when we make the calculations using the nuclear shell-model code ANTOINE [35]. For a given number of valence atoms n_v the ground-state spin is $S=\hat{n}_v/2$, with $\hat{n}_v=n_v$ if $n_v \leqslant 2l+1$ and with $\hat{n}_v=2l+1-n_v$ if $n_v>2l+1$. At midshell the state with maximum spin is unique and has $L=0$. In most other situations, we find that the ground state has $L\approx S$. The droplet develops a spin gap roughly proportional to $\hat{n}_v$ that reaches 130 mK at mid $l=5$ shell. The spin alignment is produced by the two-body interaction, and we can extract the associated correlation energy subtracting from the energy eigenvalues of the configuration mixing calculations the mean-field contribution

$$E_{mf}=\tfrac{1}{2}n(n-1)\overline{V}_{ll}, \tag{4}$$

i.e., the number of interactions times the averaged matrix element (or centroid) of the interaction that can be written as

$$\overline{V}_{ll}=\frac{l+1}{4l+1}V^0_{ll}+\frac{3l}{4l+1}V^1_{ll} \tag{5}$$

in terms of the centroids at fixed spin

$$V^S_{ij}=\frac{\sum_L (2L+1)V^{LS}_{ijij}}{\sum_L (2L+1)}. \tag{6}$$

The sums run over Pauli allowed L values. These are in fact monopole formulas currently employed in shell-model studies in nuclear physics, as given, e.g., in Ref. [36], where one has to make the correspondence between total angular momentum and orbital angular momentum ($j\rightarrow l$), and isotopic spin and spin ($t\rightarrow s$).

The resulting alignment energies are plotted in Fig. 5 for the larger l values that we have calculated. The correlation energy grows with l and with the number of valence atoms. If the Hamiltonian were purely monopolar—i.e., if the two-body matrix elements were L independent—the energy would vary quadratically with the number of atoms. What we find is a somewhat slower increase. It can also be noticed that there is some odd-even staggering, but contrary to the usual pairing regime, here an even number of atoms is unfavored. A similar trend is seen in the spin gaps, which are essentially the first derivative of the alignment energies.

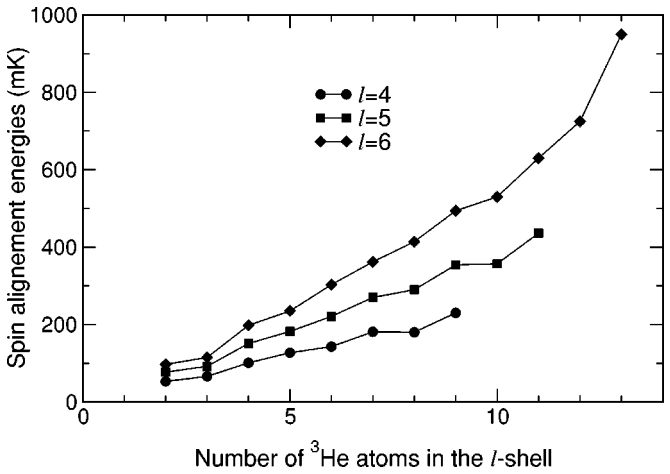

FIG. 5. Spin alignment energies as a function of the number of atoms in the l shell.

IV. SUMMARY

We have found that within a FRDF mean-field description, large enough mixed helium droplets, roughly satisfying the condition $N_3 \leqslant 3.5 N_4^{2/3}$, are formed by a core of ^{4}He atoms coated with ^{3}He atoms occupying nodeless sp states. These states have orbital angular moments running from $l=0$ to a maximum value l_m. Magic numbers characterizing shell closures appear at $N_3=2(p+1)^2$ with $p=0,1,\ldots,l_m$. For values of N_3 larger than these given by the above inequality, the fermionic equilibrium configuration, instead of being surfacelike, evolves towards a more bulky configuration, developing a plateau at a density close to the ^{3}He saturation density [12], and has a more conventional shell structure in which sp states corresponding to different radial quantum numbers n are occupied.

To incorporate the effect of correlations in one active open l shell, we have considered as residual interaction the one derived from the same density functional used to generate the mean field. We have found that, as in pure ^{3}He open-shell droplets, their two-body matrix elements are mostly attractive in the $S=1$ spin channel. Consequently, the effect of the correlations between ^{3}He atoms is to favor the alignment of spins in the *open* l shell. This is analogous to the case of pure ^{3}He open-shell droplets, although the effect in mixed droplets is less pronounced.

Finally, we would like to comment on the effect of having more than one open shell. For this sake, let us consider the case of several valence shells, i.e., configurations with n_l atoms in shell l, $n_{l'}$ atoms in shell l', and so on. If the interaction between different shells is neglected, and only intrashell interactions are taken into account, the n_l atoms would couple to spin $\hat{n}_l/2$, the $n_{l'}$ atoms to spin $\hat{n}_{l'}/2$, etc., according to the previous results. In this fictitious situation, all possible couplings between the spins of the different l shells are degenerate (as in the mean-field case). However, if intershell interactions are turned on, and one seeks for the true ground-state energy of the system, two effects compete. On the one hand, as the intershell interaction is mostly attractive in the $S=1$ channel, the lowest-energy state of this configuration would have the maximum allowed spin, namely, $\frac{1}{2}\sum_l \hat{n}_l$. On the other hand, promoting ^{3}He atoms to a higher l orbits would cost some energy. To determine which effect is the dominant one, it is unavoidable to compute the energy of these complex configurations, which represents a formidable challenge. We cannot exactly addressed this case due to the huge dimension of the m-scheme variational space—the number of Slater determinants in the space—except for a small-number of ^{3}He atoms. We have carried out exact diagonalizations for small N_3 values, and for larger N_3 values have used approximate formulas based on what in nuclear shell-model calculations are called ''monopole spin-vector'' formulas [36]. According to these calculations, the fully aligned phase is not favored. However, fairly reasonable changes in the value of the matrix elements, compatible with theoretical uncertainties in the FRDF we use for ^{3}He, might change the situation, yielding a fully polarized thin shell of ^{3}He atoms. A density-functional calculation imposing different degrees of polarization might help to shed light on this issue.

ACKNOWLEDGMENTS

This work was supported by DGI Grant Nos. BFM2000-0053, BFM2001-0208, and BFM2002-01868, and Generalitat de Catalunya Grant No. 2001SGR00064.

[1] S. Goyal, D.L. Schutt, and G. Scoles, Phys. Rev. Lett. **69**, 933 (1992).
[2] M. Hartmann, R.E. Miller, J.P. Toennies, and A.F. Vilesov, Phys. Rev. Lett. **75**, 1566 (1995).
[3] K.B. Whaley, Adv. Mol. Vib. Collision Dyn. **3**, 397 (1998).
[4] J.P. Toennies and A.F. Vilesov, Annu. Rev. Phys. Chem. **49**, 1 (1998).
[5] A. Guirao, M. Pi, and M. Barranco, Z. Phys. D: At., Mol. Clusters **21**, 185 (1991)
[6] D.M. Brink and S. Stringari, Z. Phys. D: At., Mol. Clusters **15**, 257 (1990).
[7] J. Harms, M. Hartmann, J.P. Toennies, A.F. Vilesov, and B. Sartakov, J. Mol. Spectrosc. **185**, 204 (1997).
[8] S. Grebenev, J.P. Toennies, and A.F. Vilesov, Science **279**, 2083 (1998).
[9] K.K. Lehmann and G. Scoles, Science **279**, 2065 (1998).
[10] F. Garcias, Ll. Serra, M. Casas, and M. Barranco, J. Chem. Phys. **108**, 9102 (1998); **115**, 10 154 (2001).
[11] J. Harms, M. Hartmann, B. Sartakov, J.P. Toennies, and A.F. Vilesov, J. Chem. Phys. **110**, 5124 (1999).
[12] M. Pi, R. Mayol, and M. Barranco, Phys. Rev. Lett. **82**, 3093 (1999).
[13] Ph. Sindzingre, M.L. Klein and D.M. Ceperley, Phys. Rev. Lett. **63**, 1601 (1989).
[14] M.V. Rama Krishna and K.B. Whaley, Phys. Rev. Lett. **64**, 1126 (1990).

[15] V.S. Babichenko and Yu. Kagan, Phys. Rev. Lett. **83**, 3458 (1999).
[16] W.D. Knight, K. Clemenger, W.A. deHeer, W.A. Saunders, M.Y. Chou, and M.L. Cohen, Phys. Rev. Lett. **52**, 2141 (1984).
[17] S. Tarucha, D.G. Austing, T. Honda, R.J. van der Hage, and L.P. Kouwenhoven, Phys. Rev. Lett. **77**, 3613 (1996).
[18] V.R. Pandharipande, S.C. Pieper, and R.B. Wiringa, Phys. Rev. B **34**, 4571 (1986).
[19] S. Stringari and J. Treiner, J. Chem. Phys. **87**, 5021 (1987).
[20] S. Weisgerber and P.-G. Reinhard, Z. Phys. D: At., Mol. Clusters **23**, 275 (1992).
[21] M. Barranco, D.M. Jezek, E.S. Hernández, J. Navarro, and Ll. Serra, Z. Phys. D: At., Mol. Clusters **28**, 257 (1993).
[22] M. Barranco, J. Navarro, and A. Poves, Phys. Rev. Lett. **78**, 4729 (1997).
[23] R. Guardiola and J. Navarro, Phys. Rev. Lett. **84**, 1144 (2000).
[24] R. Guardiola, Phys. Rev. B **62**, 3416 (2000).
[25] R. Guardiola and J. Navarro, Phys. Rev. Lett. **89**, 193401 (2002).
[26] D. Bressanini and G. Morosi, Phys. Rev. Lett. **90**, 133401 (2003).
[27] R. Guardiola and J. Navarro, Phys.Rev. A **68**, 055201 (2003).
[28] M. Barranco, M. Pi, S.M. Gatica, E.S. Hernández, and J. Navarro, Phys. Rev. B **56**, 8997 (1997).
[29] F. Dalfovo, Z. Phys. D: At., Mol. Clusters **14**, 263 (1989).
[30] A. Belic, F. Dalfovo, S. Fantoni, and S. Stringari, Phys. Rev. B **49**, 15 253 (1994).
[31] E. Krotscheck and R. Zillich, J. Chem. Phys. **115**, 10 161 (2001).
[32] S.M. Gatica, E.S. Hernández, and L. Szybisz, Phys. Rev. B **68**, 144501 (2003).
[33] R. Mayol, M. Barranco, E.S. Hernández, M. Pi, and M. Guilleumas, Phys. Rev. Lett. **90**, 185301 (2003).
[34] M. Moshinsky, Nucl. Phys. **8**, 19 (1958)
[35] E. Caurier, Shell Model code ANTOINE, IReS, Strasbourg, 1989 (unpublished).
[36] A. Poves and F. Nowacki, in *An Advanced Course in Modern Nuclear Physics*, Lecture Notes in Physics Vol. 581 (Springer, Berlin, 2001).